J|A|C|S COMMUNICATIONS

Published on Web 08/06/2010

Microsecond Time Scale Mobility in a Solid Protein As Studied by the ^{15}N $R_{1\rho}$ Site-Specific NMR Relaxation Rates

Alexey Krushelnitsky,*[,†] Tatiana Zinkevich,[‡] Detlef Reichert,[§] Veniamin Chevelkov,[||] and Bernd Reif[||]

Kazan Institute of Biochemistry and Biophysics, Kazan, Russia, Kazan Physical Technical Institute, Kazan, Russia, Institut für Physik - NMR, Martin-Luther-Universität Halle-Wittenberg, Halle, Germany, and Leibniz-Institut für Molekulare Pharmakologie, Berlin, Germany

Received May 1, 2010; E-mail: Krushelnitsky@mail.knc.ru

Abstract: For the first time, we have demonstrated the site-resolved measurement of reliable (i.e., free of interfering effects) ^{15}N $R_{1\rho}$ relaxation rates from a solid protein to extract dynamic information on the microsecond time scale. ^{15}N $R_{1\rho}$ NMR relaxation rates were measured as a function of the residue number in a ^{15}N,^{2}H-enriched (with 10−20% back-exchanged protons at labile sites) microcrystalline SH3 domain of chicken α-spectrin. The experiments were performed at different temperatures and at different spin-lock frequencies, which were realized by on- and off-resonance spin-lock irradiation. The results obtained indicate that the interfering spin−spin contribution to the $R_{1\rho}$ rate in a perdeuterated protein is negligible even at low spin-lock fields, in contrast to the case for normal protonated samples. Through correlation plots, the $R_{1\rho}$ rates were compared with previous data for the same protein characterizing different kinds of internal mobility.

In the past few years, solid-state NMR studies of protein dynamics have received increasing attention. Limitations in resolution in the solid state have been mostly overcome,[1,2] and liquid-state-like spectra can be recorded, clearing the way for obtaining site-specific dynamic information in the solid state. The absence of overall protein tumbling, which in solution compromises the analysis of slow internal motions, is a main advantage of solid-state investigations of molecular dynamics. Solid-state NMR experiments allow one to access the full frequency range of internal molecular motions without limitations. This is a crucial issue for revealing the role of dynamics for biological activity of proteins, since biologically important slow motions on the microsecond−millisecond−second time scale are poorly accessible in liquid-state experiments.[3]

A wide range of NMR experiments have been applied to probe the dynamics of proteins in the solid state with site-specific resolution. Different techniques are sensitive to different time scales of motion: T_1 relaxation times sample nanosecond dynamics,[4,5] line shape analysis and quantification of the motionally averaged dipolar couplings provide information on the amplitude of motions on the submicrosecond scale and faster,[6−8] and solid-state magic-angle-spinning (MAS) exchange techniques enable the characterization of slower motions on the millisecond−second time scale.[9] Internal motions taking place in the microsecond regime are still most difficult to access but can be appropriately studied by measurement of spin−lattice relaxation rates in the rotating frame ($R_{1\rho}$). In comparison with many other NMR experiments, this method has a few specific methodological difficulties. Among them are the harmful effects of the long, high-power spin-lock pulses, which cause sample heating and eventually compromise sample integrity, and the interfering spin−spin contribution to the relaxation rate. This contribution originates from the additional relaxation pathway to the lattice through the dipolar proton reservoir; this term becomes dominant at weak and moderate spin-lock fields in relatively rigid molecules.[10−12] Since the spin−spin contribution does not depend on dynamics, the $R_{1\rho}$ experiment is useless in this case for studying molecular motions. This experiment has already been applied to dynamic studies of peptides and proteins,[13−15] but to date there are practically no reports about site-specific $R_{1\rho}$ rates in totally ^{13}C- and/or ^{15}N-enriched proteins. To the best of our knowledge, we are aware of only one such paper, in which $R_{1\rho}$ rates obtained at only one temperature and one spin-lock field were used for a qualitative characterization of internal protein dynamics.[16]

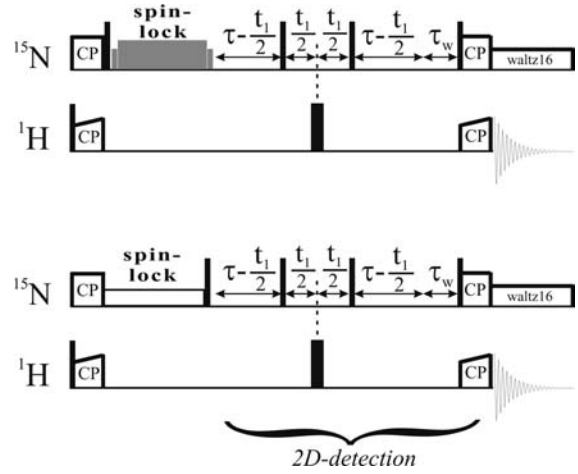

Figure 1. Pulse sequences for the (top) off-resonance and (bottom) on-resonance $R_{1\rho}$ experiments. The $R_{1\rho}$ spin-lock pulse is followed by a 2D ^{1}H,^{15}N correlation element[17] to achieve site-specific resolution. Thin and thick bars denote $\pi/2$ and π pulses, respectively. Shaded pulses indicate off-resonance irradiation. A vector diagram of the magnetization perturbations in the off-resonance experiment is shown in Figure S1. The off-resonance experiment was performed on a Bruker Avance 600 spectrometer at effective sample temperatures of 14 and 24 °C using a 4 mm MAS probe with the MAS rotation frequency adjusted to 10 kHz. The effective spin-lock field was adjusted to 34.9 kHz, yielding an angle θ between B_0 and B_{1e} on the order of 24°. The sample used in the off-resonance experiments had 20% back-exchanged protons. The on-resonance experiment was performed on a Bruker Avance 400 spectrometer at effective temperatures of 10 and 27 °C using a 3.2 mm MAS probe. The sample was spun at a MAS rotation frequency of 20 kHz with an applied on-resonance spin-lock field of 8.1 kHz. The sample used in the on-resonance experiments had 10% back-exchanged protons.

[†] Kazan Institute of Biochemistry and Biophysics.
[‡] Kazan Physical Technical Institute.
[§] Martin-Luther-Universität Halle-Wittenberg.
[||] Leibniz-Institut für Molekulare Pharmakologie.

 10.1021/ja103582n

When perdeuterated proteins are employed, proton spin interactions can be neglected; the spin−spin contribution to the relaxation rate $R_{1\rho}$ therefore vanishes, so weak spin-lock pulses can be applied. Recently, we demonstrated the advantages of using deuterated samples in which protons at labile sites are partially back-exchanged[17] in order to study molecular dynamics in the solid state.[5,8,9] This approach enables a significant enhancement of sensitivity as a result of indirect proton detection and makes proton-driven spin diffusion between ^{15}N nuclei very slow, so it does not affect T_1 relaxation and MAS exchange decays.

In this communication, we present ^{15}N $R_{1\rho}$ measurements applied to a uniformly ^{2}H,^{15}N isotopically enriched sample of the chicken α-spectrin SH3 domain in which 10−20% of the exchangeable protons at labile sites were back-substituted with protons. Experiments were carried out at different temperatures and ^{15}N effective spin-lock frequencies (8.1 and 34.9 kHz). Experiments at the higher spin-lock field were performed off-resonance in order to increase the spin-lock field without increasing the potentially dangerous RF irradiation power.[12] Figure 1 shows the pulse sequences for the off- and on-resonance $R_{1\rho}$ measurements. The sequences consist of the spin-lock relaxation time followed by a ^{1}H,^{15}N correlation element to achieve site-specific resolution.

Typical examples of the relaxation decays are shown in Figure S2 in the Supporting Information. Two reasons can account for the different fit qualities of the decays for different peaks. First, the cross-polarization efficiencies are not uniform for all of the N−H pairs, so different peaks have different intensities in the 2D correlation spectrum. Second, for the reliable determination of the relaxation rate, the relaxation time must be shorter than or at least comparable to the maximum spin-lock pulse length. However, this was not the case for all of the peaks. Increasing the length of the spin-lock pulse can affect sample integrity, and thus, we limited the length of the spin-lock pulse to 0.1−0.13 s.

The ^{15}N relaxation rates $R_{1\rho}$ as a function of the residue number are shown in Figure 2 for the two temperatures and two spin-lock

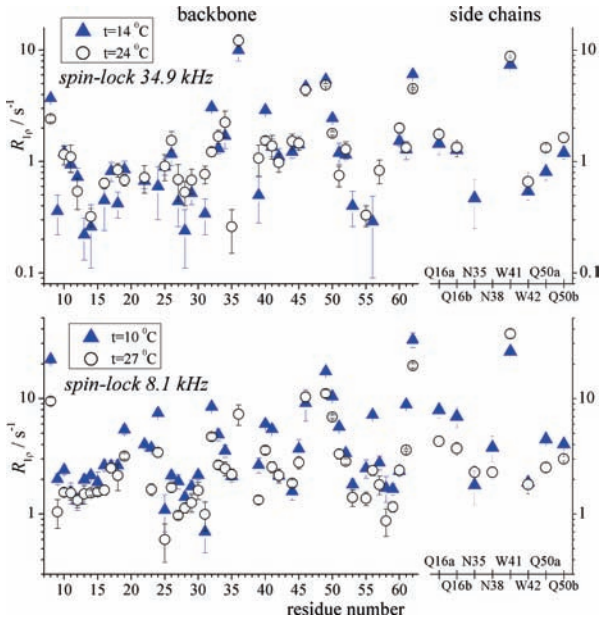

Figure 2. $R_{1\rho}$ as a function of the residue number for the (top) off-resonance and (bottom) on-resonance experiments.

fields. It is seen that the $R_{1\rho}$ values appreciably depend on temperature: for the on-resonance experiment, we found that $R_{1\rho}$(10 °C) > $R_{1\rho}$(27 °C) for most residues. This unambiguously indicates

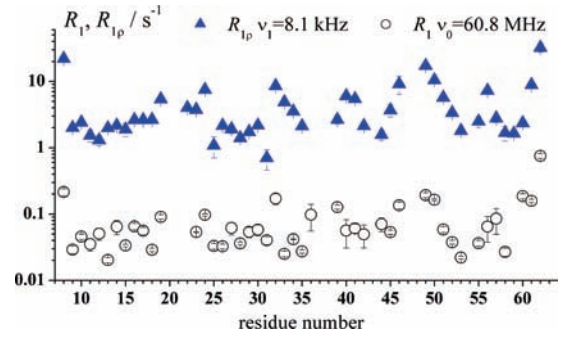

Figure 3. Values of R_1 (taken from ref 5) and $R_{1\rho}$ (from the on-resonance experiment at 10 °C) for the backbone plotted as a function of the residue number in the α-spectrin SH3 domain.

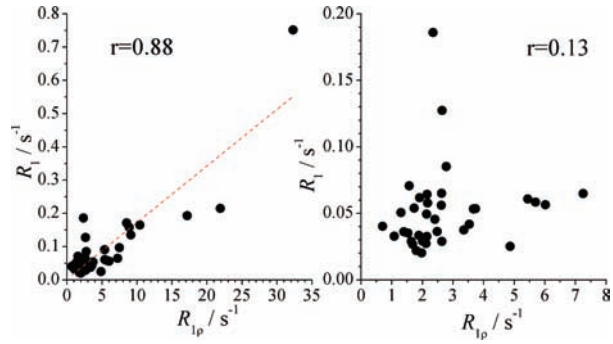

Figure 4. R_1−$R_{1\rho}$ correlation map (the data are the same as in Figure 3). The left plot includes the data for all of the backbone peaks; the right plot includes all of the data except those for residues L8, S19, T24, T32, V46, R49, Q50, L61, and D62. Values of the correlation coefficient (r) are given.

that the relaxation rates are determined (at least primarily) by molecular dynamics through the dipole−dipole and chemical shift anisotropy relaxation mechanisms. The temperature dependence in the off-resonance experiment was less pronounced, which can be explained by the smaller difference between the temperatures of the two experiments and by the higher spin-lock frequency, which appears to be close to the inverse correlation time of the motion (i.e., $R_{1\rho}$ maximum condition). The obvious variation of $R_{1\rho}$ along the backbone also confirms that the contribution of any spin-dynamics effects to the relaxation rates is negligible. Thus, deuterated samples provide $R_{1\rho}$ measurements that are free of the interfering spin−spin contribution.

In the following, we compare the $R_{1\rho}$ data with parameters characterizing protein dynamics in other frequency ranges. Figure

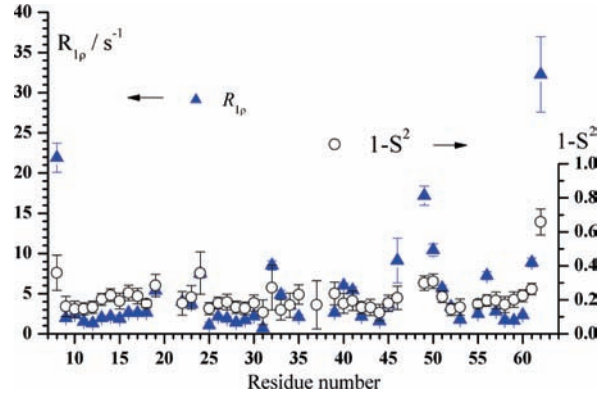

Figure 5. $R_{1\rho}$ (on-resonance experiment at 10 °C) and 1 − S^2 (order parameters S were taken from ref 8) plotted as a function of the residue number for the backbone.

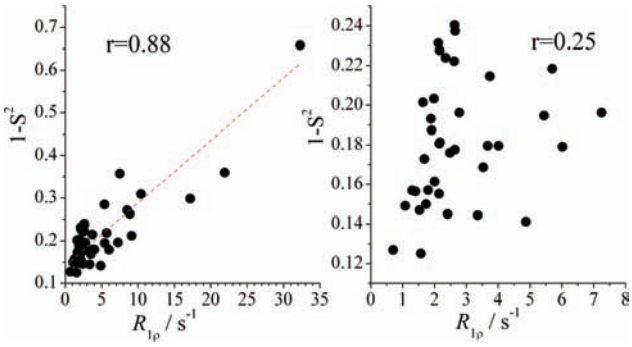

Figure 6. $R_{1\rho}-(1 - S^2)$ correlation map (the data are the same as in Figure 5). The left plot includes the data for all of the backbone peaks; the right plot includes all of the data except those for residues L8, S19, T24, T32, V46, R49, Q50, L61, and D62, as in Figure 4.

3 presents $R_{1\rho}$ and R_1 rates plotted together. $R_1 \sim J(\omega_0)$ and $R_{1\rho} \sim J(\omega_{1e})$, where $J(\omega)$ is the spectral density function and ω_0 and ω_{1e} are the resonance and spin-lock angular frequencies, which are in the megahertz and kilohertz ranges, respectively. Thus, R_1 is sensitive to the motions in the nanosecond range, while $R_{1\rho}$ reflects microsecond time scale dynamics. Figure 4 presents the same data in a form of a $R_{1\rho}-R_1$ correlation map. Clearly, residues having larger relaxation rates $R_{1\rho}$ (in comparison with the mean value) also have larger R_1 values. This applies in particular to residues L8, S19, T24, T32, V46, R49, Q50, K61, and D62. This indicates that microsecond mobility of the backbone correlates well with nanosecond motions.

A similar picture is obtained if one compares $R_{1\rho}$ and the order parameter $(1 - S^2)$ that characterizes the amplitude of all motions on the submicrosecond time scale and faster (Figure 5). This dynamic order parameter S was obtained from the site-specific solid-state NMR measurements of motionally averaged N−H dipolar couplings in the SH3 domain.[8] A correlation was observed only when residues that are known to be dynamic were included. When we excluded these nine residues, no correlation between $R_{1\rho}$ and the parameters characterizing faster dynamics was observed, as indicated by the correlation maps shown in Figure 6.

Next, we compare the internal mobility on the microsecond and millisecond−second time scales using the $R_{1\rho}$ rates and the MAS exchange NMR data, respectively. Figure 7 presents the $R_{1\rho}$ values and the recently measured dipolar CODEX data for the SH3 domain.[9] I_{start} and I_{end} refer to the CODEX signal intensities at short and long mixing times (for more details, see ref 9), and the value

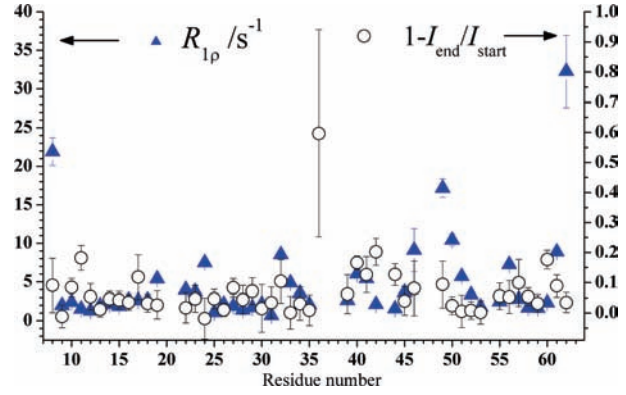

Figure 7. Relative amplitude of the decay of the mixing-time dependence for the site-resolved intensities in the dipolar CODEX experiment (the data were taken from ref 9) and the $R_{1\rho}$ data (on-resonance experiment at 10 °C) plotted as a function of the residue number for the backbone.

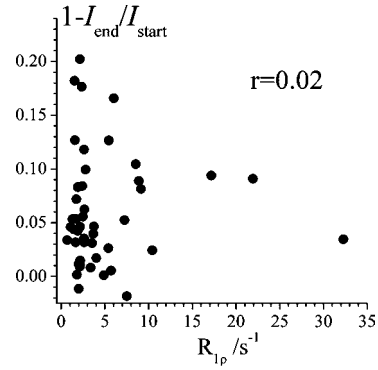

Figure 8. $R_{1\rho}-(1 - I_{end}/I_{start})$ correlation map using all of the backbone peaks (the data are the same as in Figure 7).

$(1 - I_{end}/I_{start})$ is a measure of the amplitude of slow motion. The physical meaning of this parameter is similar to that of $(1 - S^2)$. We found no correlation between microsecond and millisecond−second time scale motions (see Figure 8). The absence of the correlation between fast and slow motions was also confirmed by the $(1 - S^2)-(1 - I_{end}/I_{start})$ correlation map (Figure S3). On the other hand, the $R_{1\rho}$ and exchange data complement each other and provide a more comprehensive picture of the slow internal motions in the protein. For instance, the exchange data indicate that residues K60 and L61 located near the C-terminus of the protein have an elevated mobility on the second time scale. However, the very end of the terminal (i.e., residue D62) reveals no such mobility. At the same time, the $R_{1\rho}$ data suggest that D62 is rather mobile but on a shorter time scale (Figures 2 and 3). Thus, the combination of the exchange and $R_{1\rho}$ data demonstrates that the three terminal residues (K60, L61, and D62) undergo slow motion with a stepwise reduced correlation time toward the C-terminus of the protein.

In summary, we have demonstrated the applicability of ^{15}N on- and off-resonance $R_{1\rho}$ measurements in a microcrystalline protein to characterize internal motions with site-specific resolution. Perdeuterated samples allow the suppression of spin−spin contributions to the relaxation rate even at rather low spin-lock rf fields. The combined analysis of the $R_{1\rho}$ data and the parameters characterizing motion occurring on time scales that are shorter or longer than microseconds provides interesting correlations between mobility in various frequency ranges and gives a more comprehensive picture of the protein dynamics. A quantitative analysis of these data is under way and will be presented in future publications.

Acknowledgment. This research was supported by a grant from the Program "Molecular and Cell Biology" of the Russian Academy of Sciences, the Leibniz-Gemeinschaft, and the DFG (Re1435, SFB449, SFB740, Re 1025/16-1).

Supporting Information Available: Vector scheme of the magnetization perturbations in the off-resonance experiment, typical examples of the relaxation decays, and the $(1 - S^2)-(1 - I_{end}/I_{start})$ correlation map. This material is available free of charge via the Internet at http://pubs.acs.org.

References

(1) Hughes, C. E.; Baldus, M. *Annu. Rep. NMR Spectrosc.* **2005**, *55*, 121–158.
(2) McDermott, A. E. *Annu. Rev. Biophys.* **2009**, *38*, 385–403.
(3) Krushelnitsky, A.; Reichert, D. *Prog. Nucl. Magn. Reson. Spectrosc.* **2005**, *47*, 1–25.
(4) Giraud, N.; Blackledge, M.; Goldman, M.; Bockmann, A.; Lesage, A.; Penin, F.; Emsley, L. *J. Am. Chem. Soc.* **2005**, *127*, 18190–18201.
(5) Chevelkov, V.; Diehl, A.; Reif, B. *J. Chem. Phys.* **2008**, *128*, 052316.
(6) Hologne, M.; Faelber, K.; Diehl, A.; Reif, B. *J. Am. Chem. Soc.* **2005**, *127*, 11208–11209.

(7) Lorieau, J. L.; McDermott, A. E. *J. Am. Chem. Soc.* **2006**, *128*, 11505–11512.
(8) Chevelkov, V.; Fink, U.; Reif, B. *J. Am. Chem. Soc.* **2009**, *131*, 14018–14022.
(9) Krushelnitsky, A.; deAzevedo, E. R.; Linser, R.; Reif, B.; Saalwachter, K.; Reichert, D. *J. Am. Chem. Soc.* **2009**, *131*, 12097–12099.
(10) Vanderhart, D. L.; Garroway, A. N. *J. Chem. Phys.* **1979**, *71*, 2773–2787.
(11) Akasaka, K.; Ganapathy, S.; McDowell, C. A.; Naito, A. *J. Chem. Phys.* **1983**, *78*, 3567–3572.
(12) Krushelnitsky, A.; Kurbanov, R.; Reicher, D.; Hempel, G.; Schneider, H.; Fedotov, V. *Solid State Nucl. Magn. Reson.* **2002**, *22*, 423–438.
(13) Huster, D.; Xiao, L. S.; Hong, M. *Biochemistry* **2001**, *40*, 7662–7664.
(14) Gibson, J. M.; Popham, J. M.; Raghunathan, V.; Stayton, P. S.; Drobny, G. P. *J. Am. Chem. Soc.* **2006**, *128*, 5364–5370.
(15) Cady, S. D.; Hong, M. *J. Biomol. NMR* **2009**, *45*, 185–196.
(16) Helmus, J. J.; Surewicz, K.; Surewicz, W. K.; Jaroniec, C. P. *J. Am. Chem. Soc.* **2010**, *132*, 2393–2403.
(17) Chevelkov, V.; Rehbein, K.; Diehl, A.; Reif, B. *Angew. Chem., Int. Ed.* **2006**, *45*, 3878–3881.

JA103582N